

# UV-curable pressure sensitive adhesive films: effects of biocompatible plasticizers on mechanical and adhesion properties†

Cite this: *Soft Matter*, 2013, **9**, 6270

Sara Faraji Dana,<sup>a</sup> Duc-Viet Nguyen,<sup>b</sup> Jaspreet Singh Kochhar,<sup>a</sup> Xiang-Yang Liu<sup>bcd</sup> and Lifeng Kang<sup>\*a</sup>

We developed a new approach to fabricate pressure sensitive adhesive (PSA) hydrogel films for dermatological applications. These hydrogel films were fabricated using polyvinylpyrrolidone (PVP), poly(ethylene glycol) diacrylate (PEGDA) and polyethylene glycol (PEG) with/without propylene glycol (PG) *via* photo-polymerization. Hydrogel films with a thickness ranging from 130 to 1190  $\mu\text{m}$  were obtained. The surface morphology and drug distribution within the films were found to be uniform. The effects of different factors (polymeric composition, *i.e.*, PEG/PG presence and film thickness) on the functional properties (*i.e.*, rheological and mechanical properties, adhesion performance and drug distribution) of the films were investigated. The addition of plasticizers, namely PEG and PG, resulted in a simultaneous increase in elasticity and adhesiveness of these hydrogels, *via* the formation of hydrogen bonds, which has a direct correlation with their adhesion properties. The new approach is potentially useful for industrial applications, due to the simple procedure, precise control over film thickness, minimal usage of solvents and adjustable mechanical, rheological and adhesive properties.

Received 28th March 2013

Accepted 19th April 2013

DOI: 10.1039/c3sm50879j

[www.rsc.org/softmatter](http://www.rsc.org/softmatter)

## 1 Introduction

Pressure sensitive adhesives (PSAs) are a special class of viscoelastic polymers that adhere to the substrates of various chemical nature under the application of slight external pressure over a short period of time (1–2 seconds).<sup>1,2</sup> To be qualified as a PSA, the polymer needs a balance of elasticity and viscosity.<sup>3</sup> It should possess both relative viscous flow under applied bonding pressure, to form good adhesive contact, and cohesive strength, which are necessary for resistance to debonding stresses.<sup>4</sup> PSAs are well known and have been used for many years in a variety of medical applications, *e.g.* transdermal drug delivery patches,<sup>5–8</sup> wound healing dressings,<sup>9–11</sup> wound closures,<sup>12</sup> surgical drapes<sup>4</sup> and scaffolds for tissue

engineering.<sup>4,13</sup> The requirements of medical PSAs are challenging as they must be able to exhibit appropriate gel strength and sufficient adhesiveness against varying skin types and at the same time,<sup>14</sup> they should be easily removable from the skin surface without excessive irritation to the skin and leaving no residues on the skin. Hydrogel polymers have been used to produce medical PSAs.<sup>4</sup> The major chemical systems used for medical PSAs are acrylate based hydrogels, due to their suitable adhesive properties and a low level of skin irritation. Other polymer types, used as PSAs, include silicone-based adhesives, polyvinyl ether-based adhesives and polyvinylpyrrolidone-based adhesives.<sup>4,15</sup> In general, conventional hydrogels used as adhesives for medical applications are developed by chemical or physical crosslinkings.

Solvent-free pressure sensitive adhesives, *i.e.*, hot-melt PSAs (HMPSAs) and radiation curable PSAs, are a relatively new group of self-adhesive medical products and are of increasing importance due to environmental pressure on solvent-borne PSAs and the performance shortcomings of aqueous systems.<sup>4,15</sup> Both HMPSAs and radiation curable PSAs have grown lately due to reduced solvent consumption and waste emissions. These environmentally friendly adhesives are made from reactive compounds that contain almost no solvents (or negligible amount) or other volatile substances. In addition, photo-polymerization enables rapid conversion of monomer or macromer precursor solutions into a gel or solid under physiological conditions potentially useful for medical applications.<sup>16</sup> Photo-polymerization is simply initiated by irradiation with light, such

<sup>a</sup>Department of Pharmacy, National University of Singapore, 18 Science Drive 4, Singapore 117543, Singapore. E-mail: [lkang@nus.edu.sg](mailto:lkang@nus.edu.sg); Fax: +65 6779 1554; Tel: +65 6516 7519

<sup>b</sup>NUS Graduate School for Integrative Sciences and Engineering, National University of Singapore, Center for Life Sciences (CeLS), #05-01, 28 Medical Drive, Singapore 117456, Singapore

<sup>c</sup>Department of Physics and Department of Chemistry, National University of Singapore, 2 Science Drive 3, Singapore 117542, Singapore

<sup>d</sup>Research Institute of Biomimetics and Soft Matter, Xiamen University, Xiamen 361005, China

<sup>e</sup>College of Materials Science and Engineering, Donghua University, Shanghai 201620, China

† Electronic supplementary information (ESI) available. See DOI: 10.1039/c3sm50879j

as UV light. Even though there are many advantages in photo-polymerization, some drawbacks are still present, *e.g.* degradation upon exposure to irradiation.<sup>9</sup> By optimizing the polymerization conditions, it is possible to address the existing challenges.

Macromers and polymers, such as poly(ethylene glycol) diacrylate (PEGDA),<sup>13,17</sup> polyvinylpyrrolidone (PVP),<sup>18–20</sup> polyethylene glycol (PEG),<sup>13,19</sup> have been used previously for applications in transdermal drug delivery systems (TDDS) and tissue engineering. In medical applications, the PSA hydrogels are usually in direct contact with skin, thus the biocompatibility and non-toxicity are two major attributes to consider.<sup>11,13</sup> PVP is a well-known bioadhesive polymer with good biocompatibility and capacity for hydrogen bond formation. It has been used as one of the main components of hydrogel preparation for temporary skin covers, wound dressings or TDD patches.

To improve the mechanical properties of PVP hydrogels, plasticizers and crosslinking agents can be added.<sup>9,21</sup> PEG<sup>18,22</sup> and propylene glycol (PG),<sup>18,23</sup> as hydrophilic plasticizers, have been used to prepare hydrogels because of their hydrophilicity and biocompatibility. Plasticizers are known to cause a reduction in polymer–polymer chain secondary bonding, forming secondary bonds with the polymer chains instead.<sup>22</sup> Many of the polymers used in pharmaceutical formulations are brittle and require the addition of a plasticizer into the formulation. Plasticizers are added to pharmaceutical polymers with the intention to improve film formation and the appearance of the film, to prevent the film from cracking, to obtain desirable mechanical properties, *i.e.*, increase of elongation at break (EB), adhesiveness, toughness, film flexibility and processability and on the other hand, decrease tensile stress (TS) and hardness.<sup>24</sup> Upon addition of plasticizers, enhancement in the flexibility of polymers is the result of loosening the tightness of intermolecular forces. The plasticizers with lower molecular weight can penetrate more easily into the polymeric chains of the film forming agent, and therefore can interact with the specific functional groups of the polymer.<sup>22</sup> PG and PEG are frequently employed in TDDS to plasticize the polymeric films.<sup>18</sup>

Feldstein *et al.* reported the fabrication of PVP–PEG PSA hydrogels *via* a solvent casting technique. In this technique the high molecular weight PVP and low molecular weight PEG were crosslinked physically, *via* hydrogen bonding. Neither PVP nor PEG is individually adhesive, but the yielded hydrogels were quite adhesive due to hydrogen bonding formation. The said technique was reported to be time-consuming and the hydrogels possess poor mechanical properties (lack of elasticity).<sup>25</sup>

Crosslinking agents, *i.e.*, PEGDA,<sup>26</sup> are also added to PVP hydrogels for the improvement of the mechanical properties. As the previous studies reported, vinyl pyrrolidone (VP) and PEGDA can be radically copolymerized in the presence of a redox system by chemical crosslinking which is the formation of covalent bonds.<sup>27</sup> The yielded PVP–PEGDA product did not possess almost any adhesiveness, and also the film itself was very brittle due to the absence of hydrogen bonds and the presence of just covalent bonds (lack of viscosity).

The main drawbacks regarding these aforementioned hydrogels, both PVP–PEG and PVP–PEGDA, include their poor

mechanical properties and lack of adhesiveness, respectively. In this study, we fabricated PSA hydrogel films which benefit from both hydrogen bonds, to gain good adhesive properties, and covalent bondings, to achieve chemical crosslinking for the enhancement of mechanical strength. A photo-polymerization technique was utilized to minimize the usage of chemical solvents and fast curing.

## 2 Materials and methods

### 2.1 Materials

Poly(ethylene glycol) diacrylate (PEGDA,  $M_n$  575), 2-hydroxy-4'-(2-hydroxy-ethoxy)-2-methyl-propiophenone 98% (HHEMP) and polyvinylpyrrolidone (PVP,  $M_n$  360 000) were purchased from Sigma-Aldrich Co. (St. Louis, MO, USA). Polyethylene glycol (PEG,  $M_n$  200), and rhodamine B (Rh d B) were purchased from Alfa Aesar Co. (Heysham, Lancashire, UK). Ethanol 95% denatured with 5% methanol (EtOH) and propylene glycol (PG) were purchased from Aik Moh Paint & Chemicals Inc. (Singapore) and Shell Eastern Chemicals Co. (Singapore) respectively. All chemicals used were of reagent grade and were utilized as supplied without further purification. Ultrapure, deionised water (Millipore Direct-Q, Molsheim, France) was used in this study. The cadaver porcine skin was obtained from a local abattoir in Singapore.

### 2.2 Fabrication of pressure sensitive adhesive films

Before PSA fabrication, the glass coverslips and glass slides were immersed in 95% ethanol solution for 2 hours to clean contamination from the surface. Then, the coverslips were dried for 30 minutes at 37 °C. To fabricate PSAs, fabrication cast was prepared by using two coverslips (Technische Glaswerke Ilmenau GmbH, Germany, 130–170  $\mu\text{m}$  thickness, 22  $\times$  22 mm) supported on either edges of the same side of a glass slide as “spacers” (Continental Lab Product Inc., San Diego, CA, USA, 1–1.2 mm thickness, 25.4  $\times$  76.2 mm) and placing another coverslip on the top to create a cavity in the center, as shown in Fig. 1.

The UV crosslinkable PEGDA solutions, containing 0.5% w/w of the HHEMP photo-initiator was added to the 25% w/v solution of PVP in EtOH. To prepare different films with various adhesion properties, the PVP–PEGDA mixture was added to PG and/or PEG. The final PVP–PEGDA–PEG or PVP–PEGDA–PEG–PG precursor solutions were placed on the glass slide using a micropipette and were drawn up by capillary action into the gap between the coverslips and the glass slides. In order to obtain microfabricated pressure sensitive adhesive films with the best viscoelasticity and adhesion properties, different ratios of PVP–PEGDA–PEG and PG incorporated PVP–PEGDA–PEG were tested and finally the optimal ratios of PVP–PEGDA–PEG and PG incorporated PVP–PEGDA–PEG hydrogel films were assigned to be 1 : 7 : 2 and 1 : 7 : 2 : 0.5, respectively. The set-up was then irradiated with a high intensity UV light of 350–500 nm for 7 seconds, with a distance of 6 cm from the light source (the collimating adaptor lens), at an intensity of 12.4 W  $\text{cm}^{-2}$  using the EXFO OmniCure S200-XL UV curing station (EXFO,

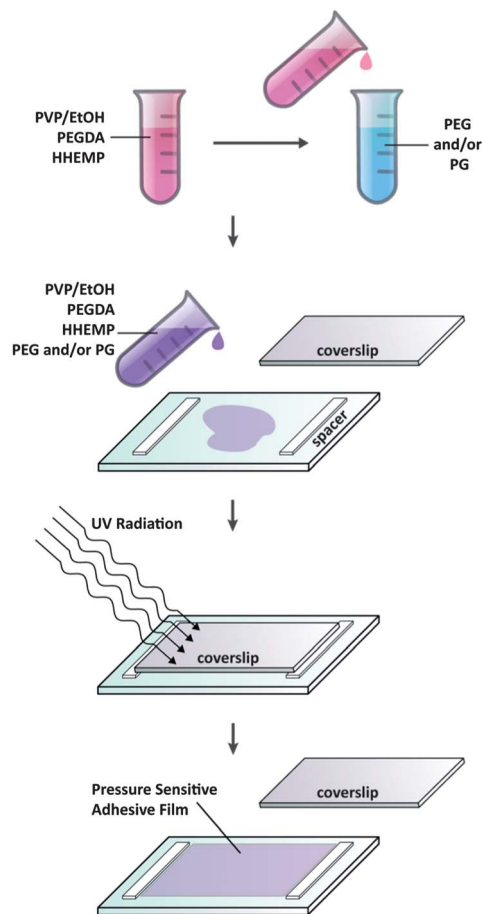


Fig. 1 The schematic representation of a PSA film fabrication process.

Photonic Solutions Inc., Canada).<sup>28</sup> The intensity of the UV light was measured with an OmniCure® R2000 radiometer. A collimating adaptor (EXFO 810-00042) was connected to the UV light guide to obtain evenly distributed light beams.

After UV irradiation, the precursor solutions exposed to UV light will be crosslinked to form PSA films, while those precursor solutions that were not exposed to UV will remain as liquid. The fabricated PSAs were developed by removing the remaining un-crosslinked precursor solutions with deionized water. Then, the coverslip was carefully removed to ensure that the formed PSA films would remain as one piece for further testing (more information is provided in the ESI† section).

### 2.3 Preparation of pig skin samples for peel tests

Pig skins excised from ear were used in our experiments. The hair of cadaver porcine ear skin were first removed using an electric hair clipper Philishave 241 (Philips, Hong Kong) followed by hair removal cream Veet (Reckitt Benckiser, Poland) to completely remove the hair.<sup>29</sup> The skin samples were gently cleaned with Kimwipe tissue paper (Kimberly-Clark, Roswell, GA, USA) and the subcutaneous fat was removed using a scalpel. The defatted skin samples were cut into small pieces (with the dimension of 30 × 50 mm) and conserved frozen at −80 °C until they were used. Prior to peel adhesion tests, the frozen skin

samples were thawed at room temperature (23 °C) for 30 minutes.<sup>30</sup> The thawed pig skin was blotted with Kimwipe tissue paper and affixed under mild tension on a glass slide using paper clips. The microfabricated pressure sensitive adhesive films were adhered to the skin with the force of a thumb before peel strength measurements were done.

All animal procedures were carried out in compliance with relevant regulations approved by the Institutional Animal Care and Use Committee (IACUC), National University of Singapore (NUS). Approval to collect the porcine skin from a local abattoir was granted by Agri-Food and Veterinary Authority (AVA) of Singapore.

## 2.4 Hydrogel characterization

**2.4.1 Morphologies of PEGDA-based hydrogels.** The microstructure and surface morphology of microfabricated hydrogel adhesive films were evaluated by Scanning Electron Microscopy (SEM, JEOL JSM-6700F) analysis operating in the high vacuum/secondary electron imaging mode at an accelerating voltage of 5 kV. The hydrogel specimens were placed in a 50 °C oven for 2 h so that the samples become completely dry prior to morphological observation. Thereafter, the hydrogel samples were sputter coated with a thin layer of platinum to improve the surface conductivity. To compare the microstructure of microfabricated hydrogel films of different compositions (PVP-PEGDA, PVP-PEGDA-PEG and PVP-PEGDA-PEG-PG films), the number of separated phases per square micrometer were counted in at least 35 subdivisions of each SEM image and averaged.

**2.4.2 Attenuated total reflection (ATR)-Fourier transform infrared (FTIR) spectroscopy.** Pure PG, PEG, PVP, PEGDA and fabricated films of PEGDA, PVP-PEGDA, PVP-PEGDA-PEG and PVP-PEGDA-PEG-PG were analyzed by ATR-FTIR to investigate their interactions. To examine the chemical structure of microfabricated hydrogel adhesive films, each film was placed on top of the crystal and a pressure arm was positioned over each sample to exert a force of ~80 N on the sample. For analysing liquid samples (*i.e.*, PEGDA, PG and PEG), a drop of liquid was placed on top of and covering the diamond crystal. No additional sample preparation was required for ATR-FTIR analysis. Removal of ethanol from prepared hydrogel films was confirmed by ATR-FTIR spectroscopy in the absence of methylene group stretching vibrations at around 2974 and 1378  $\text{cm}^{-1}$ . The ATR-FTIR spectra were acquired using a PerkinElmer Spotlight 400 FTIR Imaging System (PerkinElmer, Shelton, CT, USA) with an ATR accessory having a diamond crystal over the range of 4000–600  $\text{cm}^{-1}$  at room temperature (23 °C).

**2.4.3 Measurement of film thickness.** In the fabrication process of the pressure sensitive adhesives films, the number of spacers governs the thickness of films. Each coverslip is approximately 150  $\mu\text{m}$  thick. An increased spacer thickness was achieved by increasing the number of coverslips stacked on either side of the base glass slide as shown in Fig. 1. Depending on the number of spacers used for the fabrication (1, 3, 5 and 7 spacers), the expected thickness of films would vary from

130–170  $\mu\text{m}$  to 910–1190  $\mu\text{m}$ . The microfabricated hydrogel adhesive films were imaged using a Nikon microscope (Nikon, SMZ 1500, Tokyo, Japan) to quantify the thickness characteristics of each film. For this purpose, the thickness of each film was measured at five different sections (four corners and the middle). To show the thickness reproducibility for each film, four films with the same number of spacers were fabricated and their thickness was measured four times.

**2.4.4 Drug distribution.** To check the distribution uniformity of drugs within the PSA hydrogel films, the model drug Rhd B (0.09 wt%) was incorporated into the PEGDA-based PSA films by dissolving it in the polymer precursor solution before UV irradiation. To assess the quality of drug distribution in films, Nikon microscope (Nikon, SMZ 1500, Tokyo, Japan) and Confocal Laser Scanning Microscope (CLSM, A1R-Nikon, Tokyo, Japan) were used to capture the fluorescence cross-sectional and three-dimensional (3D) image of each film respectively. The intensity of fluorescence in each film was optically scanned at different depth intervals (2  $\mu\text{m}$ ) in three different parts (two corners and one center) using a CLSM to reconfirm the uniformity of drug distribution within PSA films.

**2.4.5 Measurements of rheological properties.** The rheological properties of the PSA hydrogels were determined using a Bohlin Gemini rotational rheometer (Bohlin Gemini HR nano, Bohlin Co., UK) equipped with 20 mm diameter parallel plates. The hydrogel film sample was placed between an upper plate fixture of a 20 mm parallel plate and a stationary surface before being subjected to sinusoidal oscillations. The gap between the two surfaces was set according to the thickness of each film.

**Dynamic strain sweep tests.** In a dynamic strain sweep test conducted at 1 Hz and 23  $^{\circ}\text{C}$ , elastic or storage modulus  $G'$  (a measure of elasticity), loss modulus  $G''$  (a measure of viscosity), and complex modulus  $G^*$  (viscoelasticity,  $G^* = [(G')^2 + (G'')^2]^{1/2}$ ) versus strain profiles were generated as strain increased from 0.0001 to 100. The linear response region or Linear Viscoelastic Region (LVER) for the dynamic frequency experiments was determined with a strain sweep, whereby a range of incremental shear stresses (1 to  $10^6$  Pa) were applied on the samples. Critical strain, the onset of hydrogel film rupture, was considered as the strain level where  $G'$  began to drop.<sup>9,31,32</sup>

**Dynamic frequency sweep tests.** The dynamic viscoelastic behaviour of hydrogels of PVP-PEGDA-PEG and PVP-PEGDA-PEG-PG was also investigated using the same rheometer. A parallel plate geometry (20 mm) was used for the measurements under small strain amplitude (0.065) to maintain the intact gel structure (within the LVER). Dynamic frequency sweep tests were carried out at 23  $^{\circ}\text{C}$  to observe  $G'$  and  $G''$  as a function of a wide range of oscillation frequencies (0.01–100 Hz). In each case, measurements were reproduced using three samples of the same composition and  $G'$  and  $G''$  were plotted vs. frequency.<sup>1</sup>

**2.4.6 Tensile tests.** Tensile tests were carried out with an Instron 5848 Microtester (Massachusetts, USA), using a 5 N load cell at room temperature (23  $^{\circ}\text{C}$ ). The hydrogel samples were cut into rectangular shapes, with a gauge length of 25 mm, width of 11 mm and different thicknesses (varied from 390–510  $\mu\text{m}$  to 910–1190  $\mu\text{m}$ ). The samples were placed between the clamps

and subjected to tension until the hydrogels lose their integrity. The tensile strain was measured as the change in the length of the film divided by the initial length of the film. The tensile stress was obtained by dividing the force by the original cross-sectional area of the film. Using these data, the stress–strain curve was plotted for each measurement to represent the mechanical properties of hydrogels.<sup>3</sup>

**2.4.7 Peel adhesion tests.** An Instron 5848 Microtester (Massachusetts, USA) was used to measure peel strengths of PSA films (11 mm width, 45 mm length, with two different thicknesses of 650  $\mu\text{m}$  and 900  $\mu\text{m}$ ) against either a rigid (glass slide) or a flexible (cadaver porcine skin) surface at room temperature (23  $^{\circ}\text{C}$ ) with a 5 N load cell. Rigid substrates (*i.e.*, glass slide) were tested for comparison with skin. The peeling adhesion testing was carried out at a rate of 50 mm  $\text{min}^{-1}$  and a peel angle of 180 $^{\circ}$ . Peel strengths were measured in triplicate, as continuous peel tests over 1 minute.<sup>33</sup> The glass slide was cleaned with acetone prior to testing to remove impurities on its surface. The skin sample was carefully wiped out with tissue paper between each peel experiment.<sup>34</sup> The outer surface of the skin was in contact with an adhesive film for testing.

## 3 Results and discussion

### 3.1 Microfabricated PSA hydrogels

Most photo-polymerization methods involve long exposure times to UV, which can potentially compromise the stability of the incorporated drugs, such as proteins, peptides, *etc.*<sup>35,36</sup> In our approach, microfabricated PSA hydrogels were obtained at a low polymerization time of 5–10 seconds which is not expected to compromise the stability of incorporated drugs (Fig. 1). This amount of time is significantly lower than that of other polymers, such as PVP, where UV-exposure up to 30 minutes has been used for fabrication of microstructures.<sup>37</sup> On the other hand, PEG-based acrylates have been shown to be crosslinked by using a wide range of exposure times<sup>38–40</sup> and factors such as polymer concentration, molecular weight, energy used, the presence of solvents, photo-initiator concentration and the presence of oxygen could influence curing properties.<sup>41</sup>

Moreover, as photo-polymeric reactions can also be influenced by the intensity of the light source used, we aimed to find the right combination of polymerization time and the UV intensity for fabricating PSA hydrogels.<sup>42</sup> It was found that a combination of a polymerization time of 7 seconds and an intensity of 12.4 W  $\text{cm}^{-2}$  was suitable for our method.

The PVP, PEGDA, PEG and PG (Fig. 2), were selected for this fabrication approach based on their biocompatibility and UV curability (PEGDA). The fabrication process involved free radical polymerization using HHEMP as the photo-initiator. Hydrophilic PEGDA macromers, which possess  $-\text{C}=\text{C}-$  bonds at their chain ends, were easily photo-crosslinked by themselves, forming a solid network through radical polymerization. The chemical crosslinkings between them lead to the formation of covalent bonds. UV irradiation of the PVP-PEGDA-PEG and PVP-PEGDA-PEG-PG polymer precursor solutions resulted in copolymerization of the monomers and the formation of white, translucent, adhesive and flexible films, presumably in which

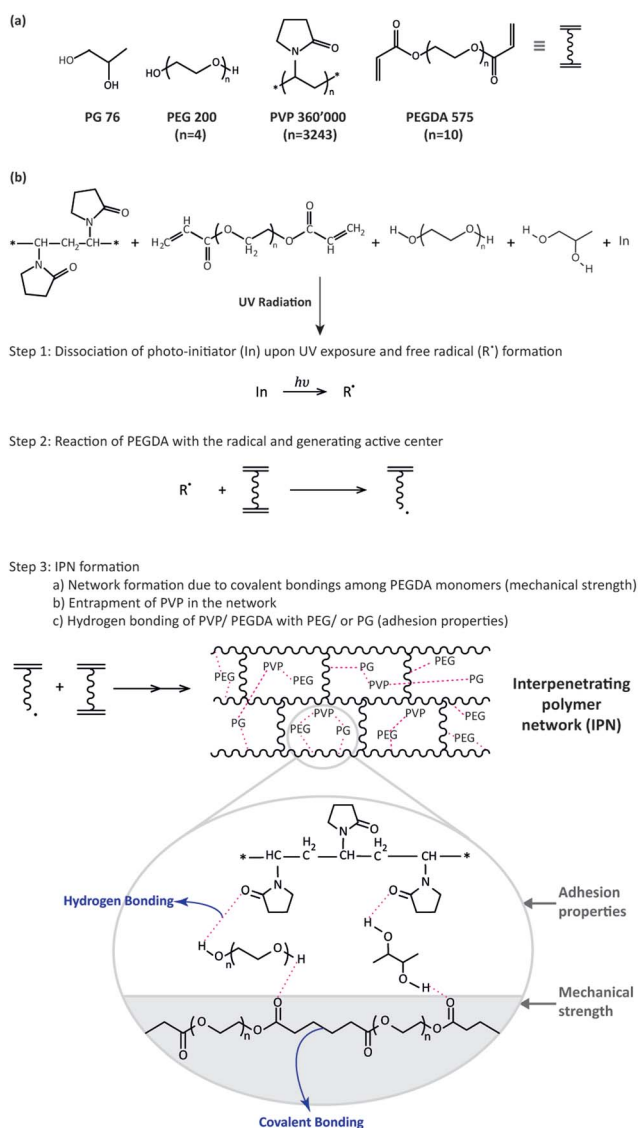


**Fig. 2** (a) Chemical structure of chemicals used for preparing PSA films, (b) proposed crosslinking mechanism for the reaction of UV-curable monomers and formation of IPN; PEGDA macromers form a crosslinked network by covalent bonding (responsible for mechanical strength) and PEGDA/PVP are bonded to PEG/ or PG *via* hydrogen bonding (responsible for adhesive properties).

PEGDAs were covalently bonded together (the reason for good mechanical strength of the film), while PG and/or PEG were physically crosslinked to PVP and/or PEGDA *via* hydrogen bonding (reason of proper adhesive properties), as both PG and PEG are hydrogen donors. According to the proposed mechanism for photo-polymerization, the HHEMP photo-initiator molecules dissociated into radicals by means of UV light absorbance at the outset of the reaction, demonstrated in Fig. 2(b). Subsequently, the formed initiator radicals reacted with the PEGDA macromer generating an active center, which could propagate through PEGDA carbon-carbon double bonds to form kinetically growing, reactive chains. It is also possible that the radical formation propagates through a pendant vinyl group of PEGDA by which a 3D polymeric network of hydrogels will form.<sup>43</sup>

As for PVP, following the UV irradiation they just get entrapped in the PEGDA 3D hydrogel network. Besides, PEGDA and entrapped PVP could be physically crosslinked with PG/ or PEG through noncovalent crosslinking which would lead to the formation of hydrogen bonding networks.<sup>27</sup> Therefore an interpenetrating polymer network (IPN) will form, composed of 3D crosslinked PEGDA network (covalent bonding), linear PVP polymer (entrapped in the 3D network), PG and/or PEG (hydrogen bonding with PEGDA/ or PVP).

Using different numbers of spacers (varied from 1 to 7), we were able to make hydrogels in different dimensions (maximum  $20 \times 22$  mm, with the thickness varying from 130  $\mu\text{m}$  to 1190  $\mu\text{m}$ ). The transparency of the films varied depending on the gel thickness. The thicker the microfabricated pressure sensitive adhesive hydrogels, the more opaque the films.

Before performing the tensile tests on the microfabricated PSA hydrogels, they were subjected to the “thumb tack test”,<sup>44</sup> (a qualitative test) for the preliminary determination of their adhesion properties. The thumb was simply pressed against the microfabricated PSA films and the relative adhesive property was evaluated. Based on the qualitative observations from the thumb tack test, it was found that the PG incorporated PVP-PEGDA-PEG microfabricated hydrogels had better adhesion properties compared to those of PVP-PEGDA-PEG, as they had more affinity to the glass slide and the resistance toward peeling off was higher. To confirm this, further tests were conducted to characterize the morphological, mechanical and rheological properties of the microfabricated films.

### 3.2 Morphological characterization by SEM

Fig. 3(a)–(c) represent the microstructure morphologies of PVP-PEGDA non-adhesive hydrogel, PVP-PEGDA-PEG and PG incorporated PVP-PEGDA-PEG microfabricated pressure sensitive hydrogels, respectively. It can be seen from these images that in comparison with the PVP-PEGDA and

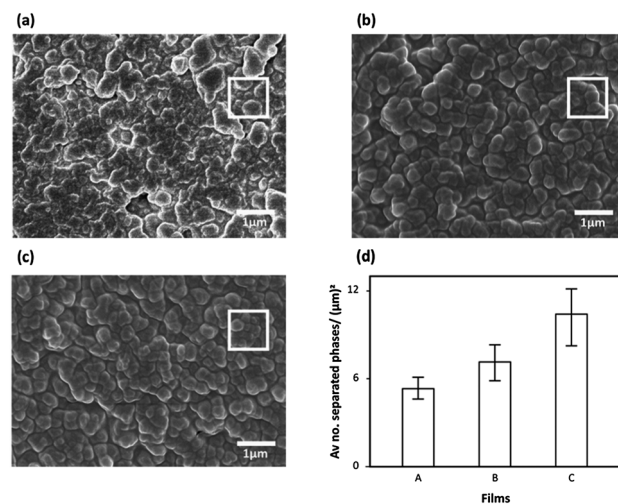


**Fig. 3** Scanning electron micrographs of (a) PVP-PEGDA, (b) PVP-PEGDA-PEG, (c) PG incorporated PVP-PEGDA-PEG copolymer PSA films and (d) comparison of an average number of separated phases per square micrometer in each film.

PVP-PEGDA-PEG hydrogels, the surfaces of the PVP-PEGDA-PEG-PG hydrogels possess a denser porous-network structure. Fig. 3(d) shows the comparison between the microstructure of microfabricated hydrogel films with different compositions (PVP-PEGDA, PVP-PEGDA-PEG and PVP-PEGDA-PEG-PG films) in regard to the existent number of separate phases per square micrometer for at least 35 subdivisions of each SEM image. It was observed that the average density of the separate phases of PVP-PEGDA films was increased by incorporating PEG and PG. From the analysis of all SEM micrographs of the fabricated hydrogels, it is shown that the morphology of films became increasingly more packed and dense by the incorporation of PEG and PEG/PG into the fabricated PVP-PEGDA hydrogels. The difference in morphology between the PVP-PEGDA-PEG and PVP-PEGDA-PEG-PG hydrogels shown in Fig. 3(b) and (c) could be explained as the influence of PG. Here, PG is performing the role of a partial crosslinking agent *via* hydrogen bonding, which causes the denser crosslinking network structure in PVP-PEGDA-PEG-PG films. These observations are also in agreement with the hypothesis that hydrogels with a maximum number of electrostatic interactions (hydrogen bonding in this case) have a tighter structure and improved network stability.<sup>45</sup>

### 3.3 Spectral characterization of dried PSA hydrogels

One of the reliable ways to detect hydrogen bonding between polymers is IR spectroscopy, in the analysis of which, a shift to lower frequencies and a drastic increase in absorbance in the frequency range of 2500–4000  $\text{cm}^{-1}$  is taken as evidence for the occurrence of hydrogen bonds involving O–H functional groups as donors and C=O as acceptors. This effect is often accompanied by the broadening of O–H and C=O stretching peaks.<sup>46,47</sup> By comparing the ATR-FTIR spectra shown in Fig. 4, an effect similar to the extensive hydrogen bond formation can be observed.

The physical crosslinking (hydrogen bonding) degree was measured from the ATR-FTIR spectra of copolymers (*i.e.*, PVP-PEGDA-PEG and PVP-PEGDA-PEG-PG) in carbonyl and hydroxyl stretching vibration regions. The degree of hydrogen bonding interactions can be deduced from changes in the peak position of the C=O stretching band (shown by dashed arrows for PEGDA and dashed circles for PVP) and the O–H stretching vibration band (shown by solid arrows), as demonstrated in Fig. 4, where hydrogen bonding is evidenced by a shift to lower wavenumbers and broadening.<sup>47,48</sup> In Fig. 4(c) and (d), the sharp band in 1690 and 1760  $\text{cm}^{-1}$  regions represents the C=O stretching band of PVP and PEGDA respectively. These bands can be attributed to carbonyl groups that are free, but bound by PVP-PVP or PEGDA-PEGDA dipole interactions. In PVP-PEGDA-PEG, Fig. 4(g) and PVP-PEGDA-PEG-PG, Fig. 4(h), although no shift to lower wavenumbers was observed, a slight broadening of C=O stretching bands was noticed, which is attributed to the C=O stretching band of either PVP or PEGDA (or both) hydrogen-bonded to PEG/or PG.<sup>49</sup>

On the other hand, the mechanical strength provided by the crosslinked PEGDA molecules is critical for PSA, particularly

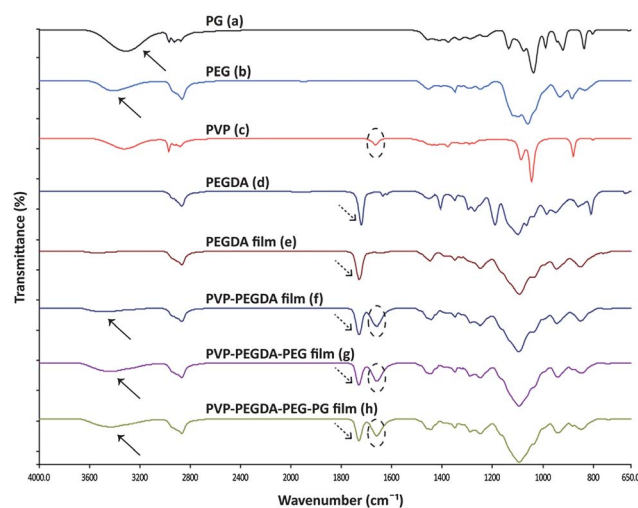


**Fig. 4** ATR-FTIR spectra of (a) PG, (b) PEG, (c) PVP, (d) PEGDA and fabricated films: (e) PEGDA, (f) PVP-PEGDA, (g) PVP-PEGDA-PEG, (h) PVP-PEGDA-PEG-PG (solid arrows, dash arrows and dash circles are attributed to hydroxyl stretching vibration band, carbonyl stretching band of PEGDA and carbonyl stretching band of PVP, respectively).

while handling the films. The covalent bonding between PEGDA molecules can be attributed to the  $\text{C}=\text{C}$ -stretching band of the acrylate group visible at 1635  $\text{cm}^{-1}$  in the un-crosslinked macromer but is lost when PEGDA molecules are photo-crosslinked (due to conversion of the carbon-carbon double bond to the carbon-carbon single bond), as seen in Fig. 4(d) and (e).<sup>13,50</sup> This phenomenon however gets masked due to the C=O stretching of PVP as shown in Fig. 4(f)–(h).

As has been established by ATR-FTIR spectroscopy of the copolymer spectra, Fig. 4(g) and (h), the physical crosslinking is due to hydrogen bonds between the proton donating hydrogen atoms of PEG/or PG terminal hydroxyl groups and the electro-negative oxygen atoms of carbonyl groups in PVP/or PEGDA.<sup>51</sup> The PG and PEG spectra, Fig. 4(a) and (b), have a broad, singlet O–H peak at around 3580–3400  $\text{cm}^{-1}$  due to one reactive OH group at each end of PG and PEG molecules. Therefore, each PG or PEG molecule is capable of forming two hydrogen bonds with the carbonyl groups in PVP/or PEGDA repeat units, acting as a physical crosslinker of PVP/or PEGDA chains. Due to hydrogen bonding, the hydroxyl stretching vibration bands of PG and PEG, Fig. 4(a) and (b), broaden and shift to lower wavenumbers,  $\sim 3700$  to 3200  $\text{cm}^{-1}$ , as observed in PVP-PEGDA-PEG (g) and PVP-PEGDA-PEG-PG (h) spectra.<sup>48</sup>

### 3.4 Control of thickness and drug distribution

The robustness of our approach to microfabrication and controlling the thickness of the polymeric films under study was evidenced by the linear relationship between the number of utilized spacers for the fabrication of the films (1, 3, 5 and 7 spacers) and their measured thickness as depicted in ESI 1(a).† ESI 1(b)† shows the thickness reproducibility for each of the four microfabricated PVP-PEGDA-PEG pressure sensitive hydrogel films with the same number of spacers (1, 3, 5 and 7 spacers).

Incorporation of Rhd B as a model drug into the PSA films during the fabrication yielded uniformly distributed micro-fabricated PVP-PEGDA-PEG-Rhd B films. This was testified by cross-sectional and three-dimensional imaging analysis of various films with different thicknesses (390–510 to 910–1190  $\mu\text{m}$ ) as shown in ESI 2(a) and (b).<sup>†</sup> Estimation of the Rhd B content by fluorescence intensity measurement at different spots of each film indicated that the model drug was distributed uniformly throughout the films, as shown in ESI 2(c).<sup>†</sup>

### 3.5 Rheological properties

In the rheological study on our PSA hydrogel films we employed both dynamic strain sweep and dynamic frequency sweep tests. In the dynamic strain sweep test, the viscoelasticity of films was measured over a wide range of shear strains (0.0001–100 strain units). Oscillatory deformation was applied to the PSA films and the material response was monitored at a constant frequency (1 Hz) and temperature (23 °C). The strain dependence of  $G'$ , as a rheological property of gels, is a measure of the brittleness and rigidity of the junctions within the structure.<sup>52</sup> Our PSA hydrogels as viscoelastic materials exhibit both elasticity of solids and viscosity of liquids. Fig. 5 shows the change of the moduli (elastic ( $G'$ ), viscous ( $G''$ ) and complex ( $G^*$ )) of the PVP-PEGDA-PEG (a) and PVP-PEGDA-PEG-PG (b) PSA hydrogel films, with the thickness of 910–1190  $\mu\text{m}$  (fabricated with 7 spacers), as functions of various oscillating strain amplitudes,  $\gamma$ . The strain corresponds to the deformation of the networks caused by the applied shear stress. The elastic modulus remains stable under small strains and decreases abruptly, *i.e.*, onset of nonlinearity, when  $\gamma$  surpasses a certain value  $\gamma_0$  (so-called critical strain) which indicates bond breakage within the networks of hydrogels.<sup>52,53</sup>

The PVP-PEGDA-PEG and PVP-PEGDA-PEG-PG micro-fabricated PSA hydrogels can withstand up to 0.5 and 0.8 of the strain, respectively. Below the critical strain, the mesh-like microstructure of the films is intact and above this, it becomes crumbled. This shows that the three-dimensional microstructure of PSA films, with or without PG in the composition, can withstand a strain up to the critical strain value, *i.e.*, 0.8 and 0.5 respectively, without showing any change in elasticity. However, the three-dimensional network cannot withstand any further increase in the applied strain and ultimately it collapses. This collapse is reflected in the decrease of the elastic modulus of the hydrogel. The length and position of the LVER of the elastic modules can be used as a measure of the stability of a PSA structure over a range of strain and as an indication of the ability to resist flow, since structural properties are best related to elasticity.<sup>31</sup>

As observed in Fig. 5(b), the PG incorporated films have longer LVER and higher critical strain values compared to films without PG incorporation, Fig. 5(a). Therefore, PG incorporated PSA films have a higher rheological stability and elasticity (flexibility).

Using the dynamic frequency sweep test, the effect of frequency on the viscoelastic properties of hydrogels as a function of time was studied. The values of  $G'$  and  $G''$  can be

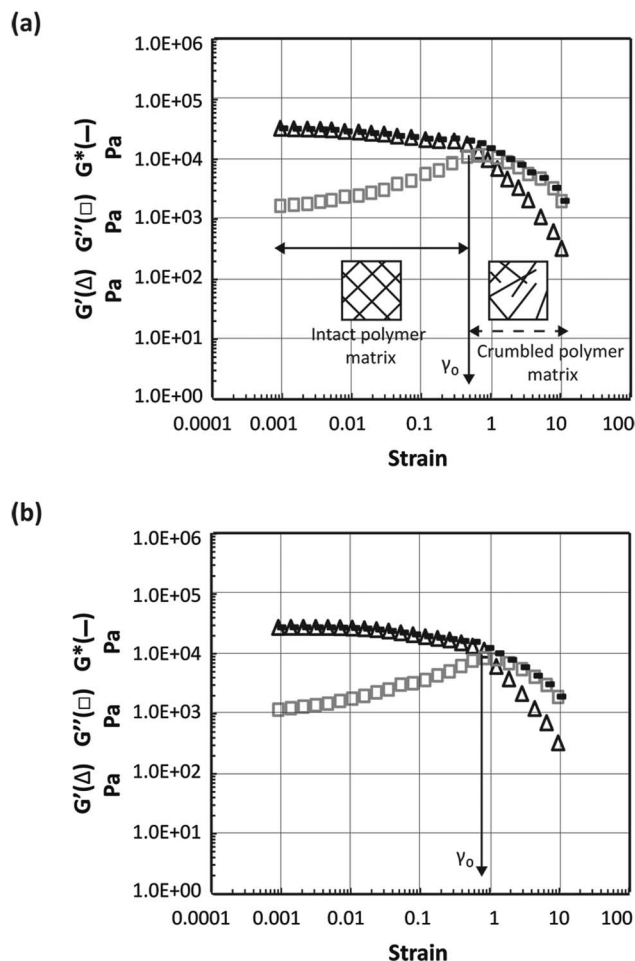


**Fig. 5** Log-log plot of shear moduli ( $G'$ ,  $G''$ ,  $G^*$ ) vs. strain for (a) PVP-PEGDA-PEG and (b) PG incorporated PVP-PEGDA-PEG copolymer PSA films with the thickness of 910–1190  $\mu\text{m}$ , fabricated with 7 spacers (frequency = 1 Hz and temperature = 23 °C).

used to confer the behaviour of PSA films under a certain strain. If  $G' > G''$ , then the material is more solid-like than liquid-like.<sup>31</sup>

The frequency sweep rheological test was done in the LVER areas (shown in Fig. 5) with a constant deformation ( $\gamma = 0.065$ ) and changing frequency from 0.1 Hz to 100 Hz. This test describes the structure type of the PSA films according to their moduli ( $G'$  and  $G''$ ).

Fig. 6(a) shows viscoelastic properties of the PVP-PEGDA-PEG hydrogels, whereas Fig. 6(b) displays the viscoelastic properties of the PG incorporated PVP-PEGDA-PEG hydrogels. For all the microfabricated PSA hydrogels,  $G'$  was greater than  $G''$  over the entire frequency range, which is consistent with the solid-like, elastic nature of the hydrogels, in other words the hydrogel behaved as a viscoelastic solid.  $G'$  and  $G''$  of the PSA hydrogels are fairly independent of frequency over a wide range of frequencies. The nearly independent and weak dependence of  $G'$  and  $G''$  with frequency, accordingly, is due to both the covalent network (chemical crosslinking) and physical nature of the network (hydrogen bonding and physical crosslinking).

Both hydrogel films, as shown in Fig. 6, retained their predominating elastic nature (up to 10 Hz of frequency) as  $G'$  are

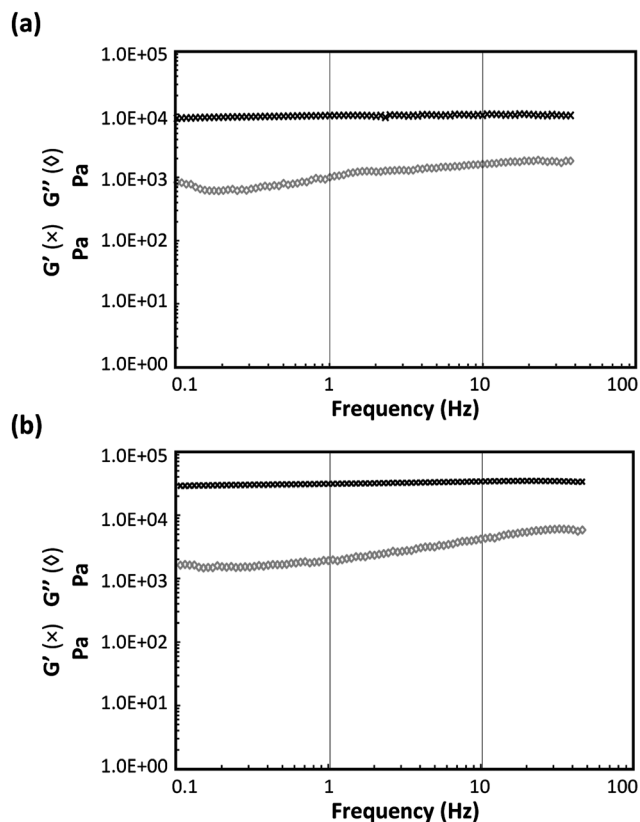


**Fig. 6** Log-log plot of average shear moduli ( $G'$  and  $G''$ ) vs. frequency for (a) PVP-PEGDA-PEG and (b) PG incorporated PVP-PEGDA-PEG copolymer PSA films with the thickness of 910–1190  $\mu\text{m}$ , fabricated with 7 spacers (strain = 0.065 and temperature = 23  $^{\circ}\text{C}$ ).

about ten times higher than  $G''$ . But, with a higher frequency of more than 10 Hz,  $G''$  gradually approach nearer to  $G'$ , shifting slightly more toward viscous nature. The upturn in  $G''$  for both hydrogel compositions, at the higher frequencies, suggests the onset of a structural change in the hydrogel network, which is most likely viscous flow.<sup>1,9</sup>

The presence of PEG and PEG-PG in the composition of the PSA films play significant roles in maintaining the viscoelasticity of the hydrogels besides the adhesion properties. Frequency sweeps over at least three decades of frequency were used to provide an indication of the type of gel formed in our PSA films as a correlation with the proposed mechanism earlier in the study. As shown in Fig. 2, we have both covalent bonds and hydrogen bonds in the structure of the microfabricated PSA hydrogels. According to the moduli trends of our microfabricated PSAs, shown in Fig. 6(a) and (b), they could be classified as a well-structured (gelled) system, due to earlier noted results (*i.e.*  $G' > G''$  and almost independent of frequency). Therefore, the PVP-PEGDA-PEG and PG incorporated PVP-PEGDA-PEG microfabricated PSA hydrogels can be considered as much of chemical (crosslinked) gels as physical (noncovalent linkages) gels. To some extent, Fig. 6 represents the effect of PG incorporation on the storage modulus ( $G'$ ), which denotes the elastic property and the loss modulus ( $G''$ ) representing the viscous property of hydrogels

with respect to frequency. From comparison of (a) and (b), it is clear that after PG incorporation  $G'$  and  $G''$  are increased. This indicates that the PG incorporated PVP-PEGDA-PEG hydrogel films are more elastic because PG is responsible to develop more physical crosslinking (hydrogen bonding) in the hydrogels.

### 3.6 Tensile testing

For the characterization of PSA films, the tensile strength and the elongation to break (EB%) are two important mechanical properties in terms of their resistance to abrasion and flexibility, respectively. Films tailored for dermatological applications must be flexible enough to follow the movements of the skin and sustain a comfortable feel, and at the same time withstand the mechanical abrasion caused by bodily movement (particularly on curved areas, such as knees and elbows) or external objects for example clothes.<sup>45,54</sup> Hence, PSA films with higher EB% (strain percentage) and TS (stress, MPa or  $\text{N mm}^{-2}$ ) are preferred for the TDD applications.

The tensile test was done on microfabricated PSA hydrogel films. Tensile stress vs. strain curves for the microfabricated PVP-PEGDA-PEG and PG incorporated PVP-PEGDA-PEG hydrogels (fabricated with 3, 5 and 7 numbers of spacers) are shown in Fig. 7(a) and (b), respectively. The PSA hydrogel films of both compositions fabricated with one spacer had a thickness range of 130–170  $\mu\text{m}$ , which were too delicate to be suitable for tensile measurements, due to difficulty in handling. Representative stress-strain curves for microfabricated PSA hydrogels with two different compositions and with 3 different thicknesses showed distinctly different profiles, although all exhibited a toe and linear elastic region and scaffolds experienced necking before deformation.

The PG incorporated PVP-PEGDA-PEG hydrogels, with 3, 5, or 7 spacers, exhibited an ultimate tensile strength of 0.06–0.12 MPa and a reasonable elongation to break of 65–85%, Fig. 7(b). The high elongation is attributed to the ability of the physical crosslinks to dissipate energy. In comparison, PVP-PEGDA-PEG, fabricated with 3, 5, or 7 spacers, demonstrated a tensile strength between 0.09 and 0.18 MPa and a percent elongation at failure between 35 and 55%. These results can be explained as a consequence of the less impacted structure and absence of PG in the structure, which made the sample more brittle and less elastic and flexible.

The hydrogel composition was shown to have an observable impact on the tensile properties of the PSAs. There is a correlation between the morphology of hydrogels and the stress-strain curves. For PG incorporated PVP-PEGDA-PEG films the morphology was more impacted with a denser distribution of the separated phases, Fig. 3(c), compared to the hydrogels without PG, Fig. 3(b). The stress-strain curve of PG incorporated PVP-PEGDA-PEG hydrogels with a more compacted structure showed approximately 1.5-fold higher tensile strain (*i.e.*, elongation) than the corresponding hydrogels without PG, as shown in Fig. 7(a) and (b) respectively.

Also by looking at each plot individually, it can be concluded that for each composition by increasing the thickness of

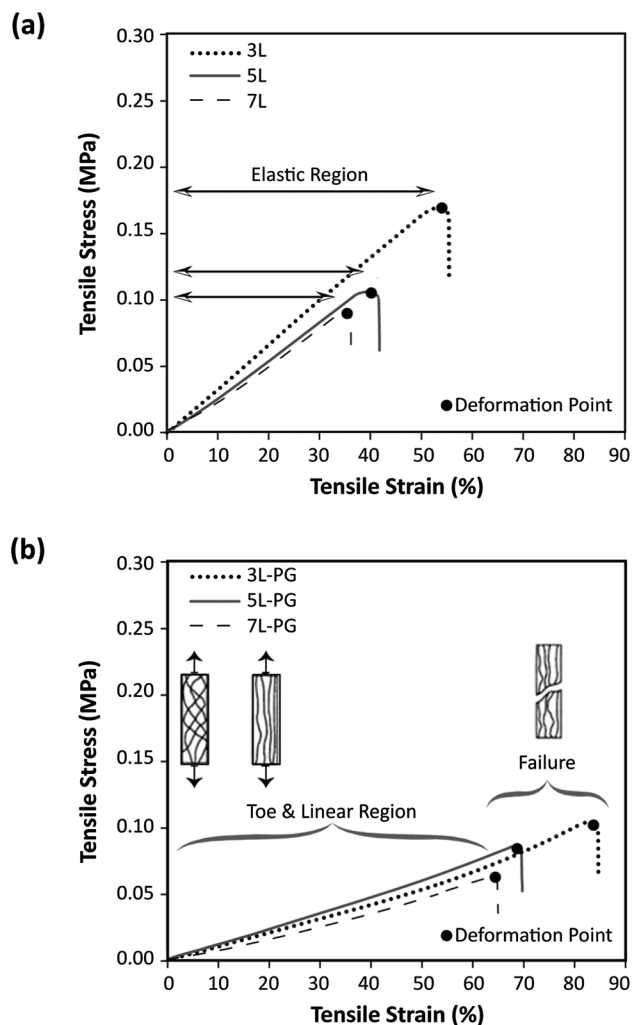


**Fig. 7** Stress-strain curve for (a) PVP-PEGDA-PEG and (b) PG incorporated PVP-PEGDA-PEG copolymer PSA films (number of spacers varied from 3 to 7).

microfabricated films from 390–510  $\mu\text{m}$  to 910–1190  $\mu\text{m}$ , the elasticity decreases and the deformation point appears earlier.

Overall, the incorporation of PG reduced the ultimate tensile stress compared to the hydrogels without PG as shown in Fig. 7(b). As expected, the ultimate tensile strain (EB%) of the PG incorporated hydrogels exhibited opposite trends compared with the ultimate stress.

Based on these evaluations, it is found that although incorporation of PG into the PSA films adversely affects the TS when compared with the films without PG, the advantage of its presence in the films by increasing EB% is more obvious which had a significant effect on the elasticity of the PSA films. A small change in the tensile stress magnitude leads to a larger change in the tensile strain percentage of PG incorporated hydrogel films, showing that they possess a larger elastic region, and the deformation occurs later (up to 85% before deformation), which makes these films more-ductile films as compared to those without PG. Enhancement of EB% by PG incorporation, as a plasticizer, may be attributed to its placement in between PVP-PEGDA polymer chains through hydrogen bonding which

spaces the polymer chains apart. This separation/spacing leads to weakening of the polymer intermolecular binding, allowing the polymer molecules to move more freely and result in the increasing flexibility of hydrogel films and a decreasing tensile strength.<sup>55,56</sup>

This indicates that the incorporation of PG into our PSA films always increases the flexibility of the films and that utilizing more number of spacers in fabrication (increase of the thickness) produces the highest increase in the EB%. It should also be noted that PVP-PEGDA-PEG films exhibit a lower flexibility when compared with PG incorporated PVP-PEGDA-PEG films with the same thickness. According to the presented results of TS and EB% attained from stress-strain curves, the PG incorporated PVP-PEGDA-PEG film with the thickness of 390–510  $\mu\text{m}$  (fabricated with 3 spacers) is the film presenting the best functional properties for the potential dermatological applications because it presents a better overall tensile strength and elasticity as it can be stretched to almost 85% of its original length.<sup>45</sup>

### 3.7 Peel testing

The peel adhesion testing was accomplished at a peel angle of 180° and a fixed rate of 50  $\text{mm min}^{-1}$ . Three different microfabricated PSA hydrogel samples of each condition (*i.e.*, change of composition and thickness) were tested. The peel strengths and the displacement of the films against both rigid (*i.e.*, glass slide) and flexible (*i.e.*, cadaver porcine skin) substrates were recorded. The maximum detachment force is noted and considered as a measure of adhesive force. The peel force of each film is plotted as a function of its displacement.<sup>6,33,44</sup>

According to the data collected, PG incorporation has a noticeable influence on the peel strengths of the microfabricated PSA films. The results of the peel testing for PVP-PEGDA-PEG and PG incorporated PVP-PEGDA-PEG films against either glass slide or skin are shown in Fig. 8(a) and (b) respectively. As can be observed from the figures, incorporation of PG into the films considerably increased the peel strengths of the PSA films compared to those without PG. The maximum peel force against glass slides was 0.79 N, 0.42 N and 0.59 N, 0.3 N against skin samples, respectively, for PSA films with PG and without PG.

The low peel strength of the PVP-PEGDA-PEG films with no PG incorporated is consistent with the morphology observed in SEM experiments. The increased number of voids present in the PVP-PEGDA-PEG films, Fig. 3(b), in other words the less packed structure of these films, lowered both the localized adhesive thickness and the contact area which leads to a reduction in the peel strength. While the PVP-PEGDA-PEG adhesive films had a similar thickness to that of the other samples (*i.e.*, PG incorporated PVP-PEGDA-PEG PSA films), due to the less dense structure, the amount of adhesive on the surface of the substrate was reduced. The reduced contact area also decreased the amount of mechanical interlocking. The combination of these properties would lower the peel strength on any PSA as it does for the PVP-PEGDA-PEG PSA films. It is

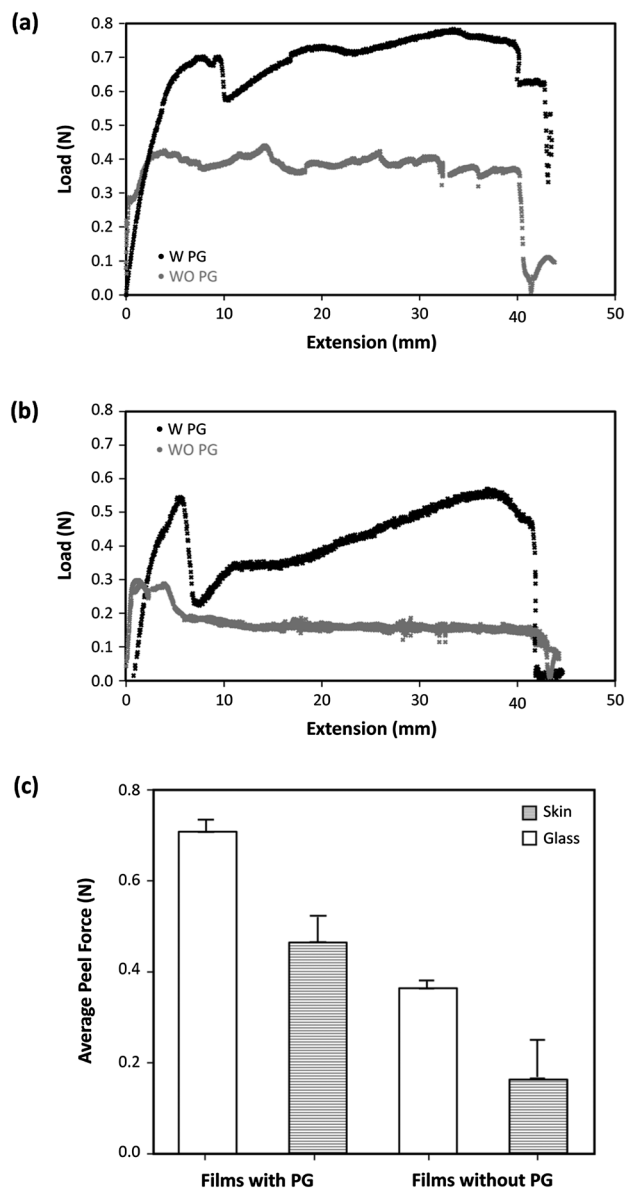


**Fig. 8** (a) PVP-PEGDA-PEG film average peel test run from a rigid substrate, glass, and a flexible one, cadaver pig skin, at a speed of  $50.00 \text{ mm min}^{-1}$ , and a nominal peel angle of  $180^\circ$ , (b) PG incorporated PVP-PEGDA-PEG film average peel test run from a rigid substrate, glass, and a flexible one, pig skin, at a speed of  $50.00 \text{ mm min}^{-1}$ , and a nominal peel angle of  $180^\circ$ . (c) Comparison of averaged  $180^\circ$  peel force for two different compositions from two different substrates.

also apparent that the peel strength of either of the compositions encounters a reduction when the substrates changed from glass to skin. As for the PG incorporated films, the maximum peel force reduced from 0.79 N to 0.59 N and for the films without PG incorporation, the maximum peel force reduced from 0.42 N to 0.3 N by switching the substrate from glass to skin.

The peel strength average of all the three measurements for each film type (PVP-PEGDA-PEG with or without PG incorporation) against both surfaces was recorded in Newton and shown in Fig. 8(c) for comparison. As noted, the PG incorporated films possess the highest peel strength against the rigid

surfaces and the PSA films without PG possess the smallest peel strength against the flexible surface.

Removal of the PSA films from different substrates involves the work done in the extension of the adhesive, distortion of the backing during the stripping action and the separation of the adhesive/surface interface.<sup>33,57</sup> As for our studies no backing layer was involved and just the adhesive films, PVP-PEGDA-PEG and PG incorporated PVP-PEGDA-PEG PSA, were used in the peeling test. The debonding of our adhesive films was *via* "Adhesive failure Case I" mode which means that when the PSA films were peeled away from either of substrates, *i.e.*, glass and cadaver pig skin, they were stripped cleanly, leaving no visible adhesive residue on the substrates.<sup>33</sup> Generally, a PSA should be able to flow into the cavities of the substrate (so-called viscosity), in order to interact tightly with the surface of the substrate.<sup>57</sup> When it makes a close contact with the surface of the substrate because of its viscoelastic properties then it will be able to make molecular interactions, such as van der Waals forces, with the skin or the substrate. The PSA-skin bonds can be built by stronger interactions (*i.e.*, hydrogen bonding), following the initial adhesion.<sup>33,57</sup> As a result, enhancements of adhesion by incorporation of PG may be attributed to the improvement of viscoelastic properties of films and hence a better wetting effect. Also these changes may be due to the enhancement of the number of hydrogen bonds in the network, as PG has two hydroxyl groups.

Besides peel strength measurements for two different compositions of films (without and with PG incorporation) against both soft and hard surfaces, the effect of varying the thickness of adhesive while keeping other factors constant was also studied. The effect of adhesive thickness, either  $650 \mu\text{m}$  or  $900 \mu\text{m}$  thick, on peel strength was almost negligible.

Thus, according to these results, it was noted that the peel force would increase with the incorporation of PG, and/or utilizing a hard substrate instead of a flexible one, but not when the film thickness changes from  $650 \mu\text{m}$  to  $900 \mu\text{m}$ .

## 4 Conclusions

To develop a suitable pressure sensitive adhesive film for dermatological applications, we devised photo-crosslinked PVP-PEGDA-PEG hydrogels. The PSA films were successfully fabricated by photo-polymerization of PVP, PEGDA and PEG polymers with/without PG. The resulted PSA hydrogel film thickness is controllable, with a densely phase-separated and uniform surface morphology. These hydrogels were capable of undergoing UV irradiation to form films in a few seconds with minimal usage of solvents compared to those prepared with conventional methods.

The PVP-PEGDA-PEG-PG films are shown to be more flexible and adhesive than the correspondent PVP-PEGDA-PEG films. Increasing the thickness of the films decreased the flexibility and elongation at break percentage of the films, but has no effect on the adhesiveness of the films. Incorporation of PG, as a plasticizer, into the PVP-PEGDA-PEG hydrogels provided the best film properties. The optimized films have shown suitable mechanical and rheological properties, *i.e.*,

flexibility, resistance and bioadhesion for dermatological applications.

## Acknowledgements

S. F. D. is a recipient of SINGA scholarship. This work was supported by a start-up grant from National University of Singapore and Singapore National Medical Research Council (NMRC) grant number: NIG09May 029. The fluorescence three-dimensional images for this study were acquired and analyzed in the SBIC-Nikon Imaging Centre at Biopolis, Singapore using a Confocal Laser Scanning Microscope. The authors would also like to thank Dr Wei Boon Teo and Ms Audrey Tay, for the assistance provided in ATR-FTIR analysis. The authors thank Maziar S. Ardejani for his stimulating discussions and Michael Abare for his careful proofreading. The authors report no conflict of interest and are solely responsible for the content of this manuscript.

## Notes and references

- 1 J. T. Padding, L. V. Mohite, D. Auhl, W. J. Briels and C. Bailly, *Soft Matter*, 2011, **7**, 5036–5046.
- 2 M. M. Feldstein, V. G. Kulichikhin, S. V. Kotomin, T. A. Borodulina, M. B. Novikov, A. Roos and C. Creton, *J. Appl. Polym. Sci.*, 2006, **100**, 522–537.
- 3 T. Wang, P. J. Colver, S. A. F. Bon and J. L. Keddie, *Soft Matter*, 2009, **5**, 3842–3849.
- 4 Z. Czech and A. Kowalczyk, in *Wide Spectra of Quality Control*, ed. I. Akyar, InTech, 1st edn, 2011, ch. 17, pp. 309–332.
- 5 K. L. Ulman and L. Chi-Long, *J. Control. Release*, 1989, **10**, 273–281.
- 6 N. Baït, B. Grassl, C. Derail and A. Benaboura, *Soft Matter*, 2011, **7**, 2025–2032.
- 7 X. Chen, W. Liu, Y. Zhao, L. Jiang, H. Xu and X. Yang, *Drug Dev. Ind. Pharm.*, 2009, **35**, 704–711.
- 8 S. Venkatraman and R. Gale, *Biomaterials*, 1998, **19**, 1119–1136.
- 9 N. Roy, N. Saha, T. Kitano and P. Saha, *Soft Mater.*, 2010, **8**, 130–148.
- 10 L. G. Ovington, *Adv. Skin Wound Care*, 2001, **14**, 259–266.
- 11 J. S. Boateng, K. H. Matthews, H. N. E. Stevens and G. M. Eccleston, *J. Pharm. Sci.*, 2008, **97**, 2892–2923.
- 12 K. W. Allen, M. Walker, R. G. Leonard, M. Brennan, K. Quigley, D. Heatley and J. F. Watts, *Anal. Proc.*, 1992, **29**, 389–398.
- 13 M. Bae, R. Divan, K. J. Suthar, D. C. Mancini and R. A. Gemeinhart, *J. Vac. Sci. Technol., B: Microelectron. Nanometer Struct. Process., Meas., Phenom.*, 2010, **28**, 24–29.
- 14 Y. Onuki, M. Hoshi, H. Okabe, M. Fujikawa, M. Morishita and K. Takayama, *J. Control. Release*, 2005, **108**, 331–340.
- 15 I. Webster, *Int. J. Adhes. Adhes.*, 1997, **17**, 69–73.
- 16 J. L. Ifkovits and J. A. Burdick, *Tissue Eng.*, 2007, **13**, 2369–2385.
- 17 A. S. Sawhney, C. P. Pathak and J. A. Hubbell, *Macromolecules*, 1993, **26**, 581–587.
- 18 S. D. Barhate, *J. Pharm. Res.*, 2009, **2**, 663–665.
- 19 A. A. Chalykh, A. E. Chalykh, M. B. Novikov and M. M. Feldstein, *J. Adhes.*, 2002, **78**, 667–694.
- 20 O. Z. Higa, S. O. Rogero, L. D. B. Machado, M. B. Mathor and A. B. Lugão, *Radiat. Phys. Chem.*, 1999, **55**, 705–707.
- 21 J. Zhang, Z. Liu, H. Du, Y. Zeng, L. Deng, J. Xing and A. Dong, *Pharm. Res.*, 2009, **26**, 1398–1406.
- 22 A. Gal and A. Nussinovitch, *Int. J. Pharm.*, 2009, **370**, 103–109.
- 23 S. Y. Lin, C. J. Lee and Y. Y. Lin, *J. Control. Release*, 1995, **33**, 375–381.
- 24 M. Rahman and C. S. Brazel, *Prog. Polym. Sci.*, 2004, **29**, 1223–1248.
- 25 M. B. Novikov, T. A. Borodulina, S. V. Kotomin, V. G. Kulichikhin and M. M. Feldstein, *J. Adhes.*, 2005, **81**, 77–107.
- 26 G. Mabilieu, I. C. Stancu, T. Honoré, G. Legeay, C. Cincu, M. F. Baslé and D. Chappard, *J. Biomed. Mater. Res., Part A*, 2006, **77A**, 35–42.
- 27 Y. Li, R. Zhang, H. Chen, J. Zhang, R. Suzuki, T. Ohdaira, M. M. Feldstein and Y. C. Jean, *Biomacromolecules*, 2003, **4**, 1856–1864.
- 28 L. Kang, M. J. Hancock, M. D. Brigham and A. Khademhosseini, *J. Biomed. Mater. Res., Part A*, 2010, **93A**, 547–557.
- 29 M. Varshney, T. Khanna and M. Changez, *Colloids Surf., B*, 1999, **13**, 1–11.
- 30 A. C. Sintov and S. Botner, *Int. J. Pharm.*, 2006, **311**, 55–62.
- 31 K. Y. Ho and K. Dodou, *Int. J. Pharm.*, 2007, **333**, 24–33.
- 32 J. L. Li, B. Yuan, X. Y. Liu and H. Y. Xu, *Cryst. Growth Des.*, 2010, **10**, 2699–2706.
- 33 A. M. Wokovich, S. Prodduturi, W. H. Doub, A. S. Hussain and L. F. Buhse, *Eur. J. Pharm. Biopharm.*, 2006, **64**, 1–8.
- 34 S. R. Trenor, A. E. Suggs and B. J. Love, *J. Mater. Sci. Lett.*, 2002, **21**, 1321–1323.
- 35 G. J. M. Fechine, J. A. G. Barros and L. H. Catalani, *Polymer*, 2004, **45**, 4705–4709.
- 36 B. A. Kerwin and R. L. Remmele, *J. Pharm. Sci.*, 2007, **96**, 1468–1479.
- 37 S. P. Sullivan, D. G. Koutsonanos, M. Del Pilar Martin, J. W. Lee, V. Zarnitsyn, S. O. Choi, N. Murthy, R. W. Compans, I. Skountzou and M. R. Prausnitz, *Nat. Med.*, 2010, **16**, 915–920.
- 38 J. S. Kochhar, S. Zou, S. Y. Chan and L. Kang, *Int. J. Nanomed.*, 2012, **7**, 3143–3154.
- 39 P. N. Desai, Q. Yuan and H. Yang, *Biomacromolecules*, 2010, **11**, 666–673.
- 40 A. Revzin, R. J. Russell, V. K. Yadavalli, W. G. Koh, C. Deister, D. D. Hile, M. B. Mellott and M. V. Pishko, *Langmuir*, 2001, **17**, 5440–5447.
- 41 D. Castro, P. Ingram, R. Kodzius, D. Conchouso, E. Yoon and I. G. Foulds, *Proceedings of MEMS 2013, IEEE 26th International Conference, Taiwan*, 2013.
- 42 J. Kindernay, A. Blažková, J. Rudá, V. Jančovičová and Z. Jakubíková, *J. Photochem. Photobiol., A*, 2002, **151**, 229–236.
- 43 G. Tan, Y. Wang, J. Li and S. Zhang, *Polym. Bull.*, 2008, **61**, 91–98.
- 44 P. Minghetti, F. Cilurzo and L. Montanari, *Drug Dev. Ind. Pharm.*, 1999, **25**, 1–6.

- 45 C. L. Silva, J. C. Pereira, A. Ramalho, A. A. C. C. Pais and J. J. S. Sousa, *J. Membr. Sci.*, 2008, **320**, 268–279.
- 46 C. P. Sherman Hsu, in *Handbook of Instrumental Techniques for Analytical Chemistry*, ed. F. A. Settle, Taylor & Francis, 1st edn, 1998, ch. 15, pp. 247–283.
- 47 P. W. Labuschagne, M. J. John and R. E. Sadiku, *J. Supercritic. Fluids*, 2010, **54**, 81–88.
- 48 M. M. Feldstein and R. A. Siegel, *J. Polym. Sci., Part B: Polym. Phys.*, 2012, **50**, 739–772.
- 49 P. Ravichandran, K. L. Shantha and K. P. Rao, *Int. J. Pharm.*, 1997, **154**, 89–94.
- 50 S. Zanini, C. Riccardi, E. Grimoldi, C. Colombo, A. M. Villa, A. Natalello, P. Gatti-Lafrancioni, M. Lotti and S. Doglia, *J. Colloid Interface Sci.*, 2010, **341**, 53–58.
- 51 M. M. Feldstein, G. A. Shandryuk, S. A. Kuptsov and N. A. Platé, *Polymer*, 2000, **41**, 5327–5338.
- 52 B. Yuan, X. Y. Liu, J. L. Li and H. Y. Xu, *Soft Matter*, 2011, **7**, 1708–1713.
- 53 L. Kang, X. Y. Liu, P. D. Sawant, P. C. Ho, Y. W. Chan and S. Y. Chan, *J. Control. Release*, 2005, **106**, 88–98.
- 54 J. Hao and R. A. Weiss, *Macromolecules*, 2011, **44**, 9390–9398.
- 55 S. Güngör, M. S. Erdal and Y. Özsoy, in *Recent Advances in Plasticizers*, ed. M. Luqman, InTech, 1st edn, 2012, ch. 5, pp. 91–112.
- 56 S. M. Lanasa, I. T. Hoffecker and S. J. Bryant, *J. Biomed. Mater. Res., Part B*, 2011, **96**, 294–302.
- 57 I. Benedek, *Pressure-Sensitive Adhesives and Applications*, Marcel Dekker Inc., 2nd edn, 2004.